MURA-547

ANALYTICAL AND COMPUTATIONAL STUDIES ON THE INTERACTION OF A SUM AND A DIFFERENCE RESONANCE

H. MEIER* AND K. R. SYMON

Midwestern Universities Research Association
Madison, Wisconsin (U.S.A.)**

*University of Wisconsin, Madison, Wisconsin.

**Supported by the United States Atomic Energy Commission.

I. Introduction

Analytical theories of the behavior of non-linear motion in two degrees of freedom near a coupling resonance lead to the conclusion[1], that near a sum resonance, there are limiting amplitudes, depending on the distance from the resonance and vanishing at the resonance, above which the coupled motion is unstable. In contrast, near a difference resonance, there are corresponding amplitudes above which the two degrees of freedom become strongly coupled and exchange 'energy', but the analytic theory predicts that the motion is stable. However, computed orbits in accelerators near difference resonances, and particularly near the 'Walkinshaw resonance' $\nu_x - 2\nu_y = 0$, have often shown[3] actual instabilities in addition to the expected strong coupling. Hagedorn[4] has offered a possible explanation of these effects as due to the presence of a pass through the potential energy hills surrounding the equilibrium point, which is not accessible to a particle moving along the x-axis or y-axis alone, even though the energy is high enough, but becomes accessible when the x and y motions are strongly coupled. We have con-

sidered the more general possibility that the paradoxial instabilities may be due to the presence of another nearby resonance in addition to the difference resonance which produces the coupling. To this end, we have chosen to consider motions for which the working point ν_x, ν_y lies near the sum resonance $\nu_x + 2\nu_y = N$ as well as the difference resonance $\nu_x - 2\nu_y = 0$. (N = number of sectors around the accelerator.) We will develop below an analytic theory of the motion, and present in addition results of fairly extensive digital computations of orbits. In order to make rapid calculations through many sectors, as well as to simplify the analytic theory, we have chosen a Hamiltonian of the simplest form which exhibits the resonance in question and which at the same time lends itself to rapid digital computation. We are able to give a partial though not a complete analytic solution to the problem. The analytic results are confirmed and extended by the results of digital computation, so that we now believe we have a fairly complete understanding of the phenomena which occur. Our explanation of the paradoxical results will be related to Hagedorn's. In our terminology, Hagedorn suggests a possible interaction between the integral resonance lines $\nu_x = 0$ and $\nu_y = 0$ and the difference resonance $\nu_x - 2\nu_y = 0$ which they intersect. This can certainly occur, but more generally the interaction may also be with other resonance lines.

The following Hamiltonian will be used for the study of the motion of a particle near the intersection (see Fig. 1) of the $\nu_x - 2\nu_y = 0$ and $\nu_x + 2\nu_y = N$ resonance lines, ($\nu_x = \frac{N}{2}$, $\nu_y = \frac{N}{4}$):

$$H = \frac{\nu_x}{2}\left(p_x^2 + x^2\right) + \frac{\nu_y}{2}\left(p_x^2 + y^2\right) - \frac{\lambda}{2}\, x\, y^2 \;\; \Delta(N\,\theta)\,. \tag{1}$$

$\Delta(N\,\theta)$ is a periodic Dirac delta function of period $\frac{2\pi}{N}$,

$$\Delta(N\,\theta) = 0 \quad \text{for} \quad \theta \neq \frac{2\pi n}{N}\,,$$

and

$$\int_{\frac{2\pi n}{N} - \varepsilon}^{\frac{2\pi n}{N} + \varepsilon} d\,\theta\;\Delta\,(N\,\theta) = 1\,,$$

where n is an integer. The horizontal and vertical displacements of the particle from the quilibrium orbit are represented by the variables x and y; the conjugate momenta, by p_x and p_y. In general the quadratic terms of an accelerator Hamiltonian will contain coefficients that are periodic in θ; however, a canonical transformation exists[1)] which will transform the accelerator Hamiltonian into a form whose quadratic terms are the same as Eq. (1).

The lowest order term in an accelerator Hamiltonian which produces resonances in the neighborhood of $\nu_x = \frac{N}{2}$, $\nu_y = \frac{N}{4}$ is $f\,(N\,\theta)\,x\,y^2$, where $f\,(N\,\theta)$ is periodic in θ with period $\frac{2\pi}{N}$. In Eq. (1), $f\,(N\,\theta)$ has been chosen as $-\frac{\lambda}{2}\Delta(N\,\theta)$. This makes it possible to express the solution of the equations of motion in the form of an algebraic transformation which will carry the particle from $\theta = \frac{2\pi n}{N}$ to $\theta = \frac{2\pi\,(n+1)}{N}$, i.e., through one sector. The function $\Delta\,(N\,\theta)$ probably perturbs the motion more than a more realistic $f\,(N\,\theta)$ for an accelerator would, since the higher harmonics of $f\,(N\,\theta)$ will go to zero while the higher harmonics of $\Delta\,(N\,\theta)$ do not. However, the qualitative features of the motion should be the same.

It has been customary (although not necessary) in computer studies of coupled motion, to compute orbits which begin with very small initial amplitudes of y-motion, and to investigate the behavior of the solution as a function of initial x-amplitude; (usually $p_x = 0$ also initially). We shall adhere to this procedure in this paper. Under these conditions, it is found both analytically and by computation that near the difference resonance there is a threshold x-amplitude x_t depending on the distance from the resonance and vanishing at the resonance, above which the y and x motion are strongly coupled and the y motion begins to grow exponentially. Analytically, the y motion should reach a maximum amplitide and decline again periodically as the 'energy' is exchanged between x and y. Computationally, it is sometimes found also to be unstable, either immediately or after a number of oscillations in amplitude. Near a sum resonance, both analysis and computation agree that there is a stability limit x_s above which the motion is unstable. We seek to study and account for these phenomena in this paper.

II. The Algebraic Transformation

From the Hamiltonian (1)

$$x' = \frac{\partial H}{\partial p_x} = \nu_x p_x ,$$

$$p'_x = -\frac{\partial H}{\partial x} = -\nu_x x + \frac{\lambda}{2} y^2 \Delta(N\theta) ,$$

and

$$y' = \frac{\partial H}{\partial p_y} = \nu_y p_y ,$$

$$p'_y = -\frac{\partial H}{\partial x} = -\nu_y y + \lambda x y \Delta(N\theta) .$$

Since the delta function occurs at $\theta = \frac{2\pi n}{N}$ the variables p_x, p_y have discontinuities at these points, while x, y are continuous:

$$
\begin{aligned}
&x\left(\frac{2\pi n}{N}+\right) = x\left(\frac{2\pi n}{N}-\right) , \\
&p_x\left(\frac{2\pi n}{N}+\right) = p_x\left(\frac{2\pi n}{N}-\right) + \frac{\lambda}{2}\, y^2\left(\frac{2\pi n}{N}\right) , \\
&y\left(\frac{2\pi n}{N}+\right) = y\left(\frac{2\pi n}{N}-\right) , \\
&p_y\left(\frac{2\pi n}{N}+\right) = p_y\left(\frac{2\pi n}{N}-\right) + \lambda\, x\left(\frac{2\pi n}{N}\right) y\left(\frac{2\pi n}{N}\right) .
\end{aligned}
\tag{2}
$$

For

$$\frac{2\pi n}{N} < \theta < \frac{2\pi(n+1)}{N} ,$$

$$x'' = \nu_x p'_x = -\nu_x^2 x ,$$

and

$$x\left(\frac{2\pi(n+1)}{N}-\right) = x\left(\frac{2\pi n}{N}+\right)\cos\frac{2\pi\nu_x}{N} + p_x\left(\frac{2\pi n}{N}+\right)\sin\frac{2\pi\nu_x}{N} ,$$

$$p_x\left(\frac{2\pi(n+1)}{N}-\right) = -x\left(\frac{2\pi n}{N}+\right)\sin\frac{2\pi\nu_x}{N} + p_x\left(\frac{2\pi n}{N}+\right)\cos\frac{2\pi\nu_x}{N} .$$

Finally, we have the transformation through a sector from $\theta = \frac{2\pi n}{N}-$ to $\frac{2\pi(n+1)}{N}-$:

$$
\begin{aligned}
x\left(\frac{2\pi(n+1)}{N}\right) &= x\left(\frac{2\pi n}{N}\right)\cos\frac{2\pi\nu_x}{N} + p_x\left(\frac{2\pi n}{N}\right)\sin\frac{2\pi\nu_x}{N} \\
&\quad + \frac{\lambda}{2}\, y^2\left(\frac{2\pi n}{N}\right)\sin\frac{2\pi\nu_x}{N} , \\
p_x\left(\frac{2\pi(n+1)}{N}\right) &= -x\left(\frac{2\pi n}{N}\right)\sin\frac{2\pi\nu_x}{N} + p_x\left(\frac{2\pi n}{N}\right)\cos\frac{2\pi\nu_x}{N} \\
&\quad + \frac{\lambda}{2}\, y^2\left(\frac{2\pi n}{N}\right)\cos\frac{2\pi\nu_x}{N} ,
\end{aligned}
\tag{3a}
$$

where we omit the minus sign, with the understanding that all variables

are evaluated just before the delta function, and in a similar manner

$$y\left(\frac{2\pi(n+1)}{N}\right) = y\left(\frac{2\pi n}{N}\right)\cos\frac{2\pi\nu_x}{N} + p_y\left(\frac{2\pi n}{N}\right)\sin\frac{2\pi\nu_x}{N} + \lambda x\left(\frac{2\pi n}{N}\right) y\left(\frac{2\pi n}{N}\right)\sin\frac{2\pi\nu_x}{N} ,$$

$$p_y\left(\frac{2\pi(n+1)}{N}\right) = -y\left(\frac{2\pi n}{N}\right)\sin\frac{2\pi\nu_x}{N} + p_y\left(\frac{2\pi n}{N}\right)\cos\frac{2\pi\nu_x}{N} + \lambda x\left(\frac{2\pi n}{N}\right) y\left(\frac{2\pi n}{N}\right)\cos\frac{2\pi\nu_x}{N} . \tag{3b}$$

With these equations a computer can calculate x, y, p_x, and p_y through a large number of sectors, several thousand times faster than it could if it had to do the calculation by solving the equations of motion numerically. An orbit can be followed through of the order of a million sectors in about an hour with the MURA IBM 704 computer. A number of computer runs have been performed based on Eqs. (3). These results will be presented in Section IV where they will be compared with the analytic results that will be derived in Section III.

III. Analytic Treatment

The analytic treatment of the problem will be based on methods developed by J. Moser[4].

Since

$$\Delta(N\theta) = \frac{N}{2\pi}\sum_{m=-\infty}^{\infty} e^{imN\theta} ,$$

then

$$H = \frac{\nu_x}{2}(p_x^2 + x^2) + \frac{\nu_y}{2}(p_y^2 + y^2) - \frac{\lambda N}{4\pi} x y^2 \sum_{m=-\infty}^{m=\infty} e^{imN\theta} . \tag{4}$$

Let

$$
\begin{aligned}
x &= \rho_{x_0}^{1/2} \cos \gamma_{x_0} , \\
p_x &= \rho_{x_0}^{1/2} \sin \gamma_{x_0} , \\
y &= \rho_{y_0}^{1/2} \cos \gamma_{y_0} , \\
p_y &= \rho_{y_0}^{1/2} \sin \gamma_{y_0} .
\end{aligned} \tag{5}
$$

The variables $\rho_{x_0}^{1/2}$, γ_{x_0} are polar coordinates in the x, p_x - phase plane, and likewise the y-variables. But also ρ_{x_0}, γ_{x_0}, ρ_{y_0}, γ_{y_0} are canonical variables with momenta ρ_{x_0}, ρ_{y_0}. The Hamiltonian is $K_0 = -2H$:

$$
K_0 = -\nu_x \rho_{x_0} - \nu_y \rho_{y_0} + \frac{\lambda N}{2\pi} \rho_{x_0}^{1/2} \rho_{y_0} \cos \gamma_{x_0} \cos^2 \gamma_{y_0} \sum_{m=-\infty}^{m=\infty} e^{imN\theta} ,
$$

or

$$
\begin{aligned}
K_0 = -\nu_x \rho_{x_0} - \nu_y \rho_{y_0} + \frac{\lambda N}{8\pi} \rho_{x_0}^{1/2} \rho_{y_0} \sum_{m=-\infty}^{\infty} \Big[& 2 \cos(\gamma_{x_0} + mN\theta) \\
& + \cos(\gamma_{x_0} + 2\gamma_{y_0} + mN\theta) + \cos(\gamma_{x_0} - 2\gamma_{y_0} + mN\theta) \Big] .
\end{aligned} \tag{6}
$$

We now make a transformation $\rho_{x_0}, \gamma_{x_0}, \rho_{y_0}, \gamma_{y_0} \rightarrow \rho_x, \gamma_x, \rho_y, \gamma_y$ by means of the generating function

$$
\begin{aligned}
S = {} & \gamma_{x_0} \rho_x + \gamma_{y_0} \rho_y \\
& - \frac{\lambda N}{8\pi} \rho_x^{1/2} \rho_y \Bigg[\sum_{\substack{m \neq 1 \\ m=-\infty}}^{\infty} \frac{\sin(\gamma_x + 2\gamma_y + mN\theta)}{(mN - \nu_x - 2\nu_y)} \\
& \qquad + \sum_{\substack{m=-\infty \\ m \neq 0}}^{\infty} \frac{\sin(\gamma_x - 2\gamma_y + mN\theta)}{(mN - \nu_x + 2\nu_y)} + \sum_{m=-\infty}^{\infty} \alpha \frac{\sin(\gamma_x + mN\theta)}{(mN - \nu_x)} \Bigg] ,
\end{aligned} \tag{7}
$$

to obtain the new Hamiltonian

$$
\begin{aligned}
K = {} & -\nu_x \rho_x - \nu_y \rho_y \\
& + \frac{\lambda N}{8\pi} \rho_x^{1/2} \rho_y \left[\cos(\gamma_x + 2\gamma_y + N\theta) + \cos(\gamma_x - 2\gamma_y) \right] + \cdots ,
\end{aligned} \tag{8}
$$

where the dots contains terms of higher order than $\rho_x^{1/2} \rho_y$. The

coefficients of these terms are small if (ν_x, ν_y) is closer to $(\frac{N}{2}, \frac{N}{4})$ than to any other intersection of resonance lines excited by $-\frac{\lambda}{2} x y^2 \Delta(N\theta)$. Fig. 1 shows the lines excited by this term, (solid lines), as well as other nearby resonances which are important in accelerators and may be excited by terms of other forms which we have not included. Some of these resonances are driven by higher order terms represented by the dots in Eq. (8).

A typical term, for example, appearing in K which might be important near the point $\nu_x = \frac{N}{2}$, $\nu_y = \frac{N}{4}$ is approximately

$$-\frac{\lambda^2}{768}\left[\frac{\epsilon_-(1-.342\,\epsilon_-^2)}{(1-\epsilon_-^2)} + \frac{\epsilon_+(1-.342\,\epsilon_+^2)}{(1-\epsilon_+^2)}\right]\rho_y^{\,2}\cos(4\gamma_y + N\theta),$$

where

$$\epsilon_+ = \nu_x + 2\nu_y - N,$$

$$\epsilon_- = \nu_x - 2\nu_y$$

measure the distance of the working point ν_x, ν_y from the sum and the difference resonance. Note that since $\epsilon_+ = \epsilon_- = 0$ for $\nu_x = \frac{N}{2}$, $\nu_y = \frac{N}{4}$, the term vanishes at this point. This term would tend to drive the resonance $\nu_y = \frac{N}{4}$, which passes through $\nu_x = \frac{N}{2}$, $\nu_y = \frac{N}{4}$.

It will be assumed that ρ_x and ρ_y are small enough, and the operating point is close enough to $\nu_x = \frac{N}{2}$, $\nu_y = \frac{N}{4}$ so that all terms in K of order ρ^2 and higher can be neglected, and K will be set equal to

$$K = -\nu_x\rho_x - \nu_y\rho_y + \frac{\lambda N}{8\pi}\rho_x^{1/2}\rho_y\left[\cos(\gamma_x + 2\gamma_y + N\theta) + \cos(\gamma_x - 2\gamma_y)\right]. \qquad (9)$$

Note that we can obtain Eq. (9) immediately simply by neglecting all non-linear terms in Eq. (6) except those which excite the two resonances

It is not necessary to know y and p_y in terms of $\underline{\rho}_x$, $\underline{\rho}_y$, $\underline{\gamma}_x$, and $\underline{\gamma}_y$. The only information needed is that if $\underline{\rho}_y$ is very small then y and p_y are very small, and conversely. However, to order $\rho_x^{1/2}$, $\rho_y^{1/2}$, we may identify $\underline{\rho}_x, \underline{\gamma}_x, \underline{\rho}_y, \underline{\gamma}_y$ with $\rho_{x0}, \gamma_{x0}, \rho_{y0}, \gamma_{y0}$ in Eqs. (5) at $\theta = \frac{8\pi n}{N}$.

Since $\underline{K}$ does not contain θ explicitly it is a constant of the motion. $\underline{K}$ can also be written in the form

$$\underline{K} = -\epsilon_x \underline{\rho}_x - \epsilon_y \underline{\rho}_y + \frac{\lambda N}{4\pi} \underline{\rho}_x^{1/2} \underline{\rho}_y \cos \underline{\gamma}_x \cos 2\underline{\gamma}_y , \tag{13a}$$

where

$$\epsilon_x = \nu_x - \frac{N}{2} , \quad \epsilon_y = \nu_y - \frac{N}{4} .$$

It is convenient to reintroduce rectangular coordinates in the rotating x- and y-phase planes:

$$X = \underline{\rho}_x^{1/2} \cos \underline{\gamma}_x , \qquad Y = \underline{\rho}_y^{1/2} \cos \underline{\gamma}_y ,$$
$$P_x = \underline{\rho}_x^{1/2} \sin \underline{\gamma}_x , \qquad P_y = \underline{\rho}_y^{1/2} \sin \underline{\gamma}_y .$$

In these rectangular coordinates,

$$-\frac{1}{2}\underline{K} = \frac{1}{2}\epsilon_x P_x^2 + \frac{1}{2}\left(\epsilon_y + \frac{\lambda N}{4\pi} X\right) P_y^2 + \frac{1}{2}\epsilon_x X^2 + \frac{1}{2}\epsilon_y Y^2 - \frac{\lambda N}{8\pi} X Y^2 . \tag{13b}$$

Let us first take ϵ_x, ϵ_y in the first quadrant (both positive, see insert Fig. 1). Eq. (13b) can be regarded as a Hamiltonian in which the first two terms represent a positive definite kinetic energy (if $X > -\frac{4\pi\epsilon_y}{\lambda N}$), and the last three, a potential energy V (X, Y). The potential V (X, Y) contains a valley from which the particle may exit through either of two passes whose saddle points lie at

$$X_s = \frac{4\pi}{\lambda N}\epsilon_y , \quad Y_s = \pm \frac{4\pi}{\lambda N}(2\epsilon_x \epsilon_y)^{1/2} ,$$

and the minimum energy for crossing either pass is

$$-\frac{1}{2}K_\ell = \frac{1}{2}\epsilon_x \epsilon_y^2 \left(\frac{4\pi}{\lambda N}\right)^2 .$$

For negligible initial y-amplitude, and $p_x = 0$ initially, the limiting x-amplitude for which the energy is sufficient to cross the pass is

$$|x_\ell| = X_\ell = \frac{4\pi}{\lambda N}\left(\nu_y - \frac{N}{4}\right). \tag{14}$$

Note that at this amplitude, the 'mass' of the y-motion can become zero and at greater energies the particle can escape via the point $-X_\ell, y=0$ by acquiring a negative y-mass as well as over the passes at X_ℓ, $\pm Y_\ell$.

Our analysis does not indicate under what conditions the particle will escape if initially $|x| > X_\ell$, but only that if $|x| < X_\ell$ it surely cannot escape (to the extent that the Hamiltonian (13) is a valid approximation). We shall have more to say later as to when it actually does escape. In view of the asymptotically convergent character of the Moser-Birkhoff solution by successive transformations, we may expect that our statements based on the Hamiltonian (13) are valid for very long times for small enough amplitudes. Since we find a structure of the dynamical motions with a scale proportional to the distances from the resonances, by going near enough the fixed point, we may expect to find this structure reproduced as accurately as we wish.

If we now consider the second quadrant ($\epsilon_x < 0, \epsilon_y > 0$) we readily observe that our Hamiltonian (13b) is no longer positive (or negative) definite even near the origin, and we can find curves of constant K = 0 connecting the origin with infinity. We can therefore say nothing about

the stability in this case, except that it is 'energetically' possible with the Hamiltonian (13b) for the particle to escape with any initial amplitude.

We will prove later a theorem of corresponding motions, a corollary of which is that motions in the third and fourth quadrants are identical with those for corresponding working points in the first and second quadrants.

We can give a complete solution for the motion if we treat the effect of a single resonance separately. Let us take the difference resonance, $\nu_x - 2\nu_y = 0$. We could transform away the term in the Hamiltonian (11) which drives the sum resonance, or, more easily, simply neglect it, which is equivalent to equating the new and old variables in the transformation:

$$\underline{K} = -(\nu_x - \tfrac{N}{2})\underline{\rho}_x - (\nu_y - \tfrac{N}{2})\underline{\rho}_y + \frac{\lambda N}{8\pi}\underline{\rho}_x^{1/2}\underline{\rho}_y \cos(\underline{\gamma}_x - 2\underline{\gamma}_y) . \tag{15}$$

Now the generating function

$$S = \rho_1(\underline{\gamma}_x - 2\underline{\gamma}_y) + \rho_2\underline{\gamma}_y$$

leads to the transformation

$$\underline{\rho}_x = \frac{\partial S}{\partial \underline{\gamma}_x} = \rho_1 , \quad \underline{\rho}_y = \rho_2 - 2\rho_1 ,$$

$$\gamma_1 = \underline{\gamma}_x - 2\underline{\gamma}_y , \quad \gamma_2 = \underline{\gamma}_y ,$$

$$K_1 = -(\nu_x - 2\nu_y)\rho_1 - (\nu_y - \tfrac{N}{4})\rho_2 + \frac{\lambda N}{8\pi}\rho_1^{1/2}(\rho_2 - 2\rho_1)\cos\gamma_1 . \tag{16}$$

Since γ_2 is ignorable,

$$\frac{d\rho_2}{d\theta} = -\frac{\partial K_1}{\partial \gamma_2} = 0 ,$$

ρ_2 is a constant, and terms containing ρ_2 only can be absorbed in K_1, since K_1 is also a constant of the motion. K_1 can be written

$$K_1 = -\epsilon_- \rho_1 + \frac{\lambda N}{8\pi} \rho_1^{1/2} (\rho_2 - 2\rho_1) \cos \gamma_1 , \tag{17}$$

where ϵ_- measures the distance from the resonance, as defined previously.

We finally transform back to rectangular variables

$$\begin{aligned} X &= \rho_1^{1/2} \cos \gamma_1 , \\ P_X &= \rho_1^{1/2} \sin \gamma_1 , \end{aligned} \tag{18}$$

and

$$H_1 = -\tfrac{1}{2} K_1 = \tfrac{1}{2} \epsilon_- (X^2 + P_X^2) - \frac{\lambda N}{16\pi} X (\rho_2 - 2X^2 - 2P_X^2) . \tag{19}$$

Fixed points occur when $\partial H_1 / \partial X = \partial H_1 / \partial P_X = 0$,

$$\left[\epsilon_- + \frac{\lambda N}{4\pi} X \right] P_X = 0 , \tag{20}$$

$$-\frac{\lambda N}{16\pi} \rho_2 + \epsilon_- X + \frac{3\lambda N}{8\pi} X^2 + \frac{\lambda N}{8\pi} P_X^2 = 0 . \tag{21}$$

Four fixed points exist:

$$\begin{aligned} X_{\pm}^{(1)} &= \frac{-\epsilon_- \pm \left[\epsilon_-^2 + \frac{3\lambda^2 N^2}{32\pi^2} \right]^{1/2}}{3\lambda N / 4\pi} , \\ P_X^{(1)} &= 0 , \end{aligned} \tag{22}$$

and

$$\begin{aligned} X^{(2)} &= -\frac{4\pi}{\lambda N} \epsilon_- , \\ P_{X\pm}^{(2)} &= \pm \left[\tfrac{1}{3} \rho_2 - \frac{16\pi^2}{\lambda^2 N^2} \epsilon_-^2 \right]^{1/2} . \end{aligned} \tag{23}$$

From equation (16) ρ_2 is always positive, and P_x is real, hence the fixed points given by equation (23) occur only for

$$\rho_2 \geq \frac{32\pi^2}{\lambda^2 N^2} \epsilon_-^2 . \tag{24}$$

Also, from equation (16) it can be seen that

$$\rho_1 \leq \frac{1}{2}\rho_2 \tag{25}$$

With the aid of Eqs. (22), (23), (24), and (25) phase plots in X, P_x can be drawn. (See Fig. 2.)

Case (i) $\rho_2 < \frac{32\pi^2}{\lambda^2 N^2} \epsilon_-^2$.

According to Eq. (24) only the fixed points $P_x^{(1)}$, $X_\pm^{(1)}$ occur. Also, from Eq. (25)

$$\rho_1 < \frac{16\pi^2}{\lambda^2 N^2} \epsilon_-^2 ,$$

and

$$|X| < \rho_1^{1/2} ,$$

but from Eq. (22)

$$|X^{(1)}| > \rho_1^{1/2} ,$$

so it is in the excluded region, and the phase plot appears as in Fig. 2a.

Case(ii) $\rho_2 > \frac{32\pi^2}{\lambda^2 N^2} \epsilon_-^2$.

In this case all four fixed points are present and the phase plot appears as in Fig. 2b. From Eq. (16) we see that if we take as initial conditions $\rho_y \ll \rho_x$, the point will follow a path in phase space which is very close to the circle $\rho_1 = \frac{1}{2}\rho_2$. In diagram 5a the path remains close

to the circle and there is no change in the nature of the motion. In diagram 5b there is a sudden change leading to y growth at the fixed points $\rho_{x\pm}^{(2)}, X^{(2)}$. Hence the condition for y growth is that for $\rho_y \ll \rho_x$ initially,

$$\rho_1 \doteq \frac{1}{2}\rho_2 > \frac{16\pi^2}{\lambda^2 N^2}(\nu_x - 2\nu_y)^2,$$

and if p_x is initially zero, the threshold for y-growth is

$$x_t = \rho_x^{1/2} = \rho_1^{1/2} = \frac{4\pi}{\lambda N}|\nu_x - 2\nu_y|. \tag{26}$$

This means that if one starts the motion with y and p_y very small, $p_x = 0$, and $|x| < x_t$, then y will remain very small. However, if $|x| > x_t$, then no matter how small y is, so long as it is not zero, it will grow large. Note that the y amplitude does not grow indefinitely but exhibits a periodic oscillation to a finite amplitude which can be calculated:

$$\rho_{y\,max}^{1/2} = \left[2(x_0^2 - x_t^2)\right]^{1/2}, \tag{27}$$

where x_0 is the initial x-amplitude. This result is confirmed by numerical computations in appropriate cases, as we shall see.

In the case where the sum resonance, $\nu_x + 2\nu_y = N$ acts alone, we can follow a similar procedure and again give a complete description of the motion. The phase plots in appropriate coordinates are in fact just the outside (cross hatched) regions in Figs. 2. We will limit ourselves to quoting the result for the case of interest, namely, very small initial y-amplitude, and p_x initially zero, for which we find a

stability limit

$$x_s = \frac{4\pi}{\lambda N} |\nu_x + 2\nu_y - N| . \tag{28}$$

If initially $|x| < x_s$, the motion is stable, but if $|x| > x_s$, the y-amplitude and likewise the x-amplitude grow without limit.

If the Hamiltonian given by Eq. (10) were exact, a theorem of corresponding motions would hold. Let

$$K = -\alpha \epsilon_x \rho_x - \alpha \epsilon_y \rho_y + A \rho_x^{1/2} \rho_y \left[\cos(\gamma_x + 2\gamma_y) + \cos(\gamma_x - 2\gamma_y)\right] . \tag{29}$$

The equations of motion are

$$\begin{aligned}
\frac{d\rho_x}{d\theta} &= A \rho_x^{1/2} \rho_y \left[\sin(\gamma_x + 2\gamma_y) + \sin(\gamma_x - 2\gamma_y)\right], \\
\frac{d\rho_y}{d\theta} &= 2A \rho_x^{1/2} \rho_y \left[\sin(\gamma_x + 2\gamma_y) - \sin(\gamma_x - 2\gamma_y)\right], \\
\frac{d\gamma_x}{d\theta} &= -\alpha \epsilon_x + \frac{A \rho_y}{2\rho_x^{1/2}} \left[\cos(\gamma_x + 2\gamma_y) + \cos(\gamma_x - 2\gamma_y)\right], \\
\frac{d\gamma_y}{d\theta} &= -\alpha \epsilon_y + A \rho_x^{1/2} \left[\cos(\gamma_x + 2\gamma_y) + \cos(\gamma_x - 2\gamma_y)\right].
\end{aligned} \tag{30}$$

Now let

$$\underline{\theta} = \alpha \theta , \qquad \rho_x = \alpha^2 \underline{\rho}_x , \quad \gamma_x = \underline{\gamma}_x$$

$$\frac{d}{d\theta} = \alpha \frac{d}{d\underline{\theta}} , \quad \rho_y = \alpha^2 \underline{\rho}_y , \quad \gamma_y = \underline{\gamma}_y$$

Then

$$\frac{d\underline{\rho}_x}{d\underline{\theta}} = A \underline{\rho}_x^{1/2} \underline{\rho}_y \left[\sin(\underline{\gamma}_x + 2\underline{\gamma}_y) + \sin(\underline{\gamma}_x - 2\underline{\gamma}_y)\right],$$

$$\frac{d}{d\underline{\theta}}\underline{\rho}_y = 2A\underline{\rho}_x^{1/2}\underline{\rho}_y\left[\sin(\underline{\gamma}_x+2\underline{\gamma}_y)-\sin(\underline{\gamma}_x-2\underline{\gamma}_y)\right],$$

$$\frac{d}{d\underline{\theta}}\underline{\gamma}_x = -\epsilon_x + \frac{A\underline{\rho}_y}{2\underline{\rho}_x^{1/2}}\left[\cos(\underline{\gamma}_x+2\underline{\gamma}_y)+\cos(\underline{\gamma}_x-2\underline{\gamma}_y)\right],$$

$$\frac{d}{d\underline{\theta}}\underline{\gamma}_y = -\epsilon_y + A\underline{\rho}_x^{1/2}\left[\cos(\underline{\gamma}_x+2\underline{\gamma}_y)+\cos(\underline{\gamma}_y-2\underline{\gamma}_y)\right]. \tag{31}$$

These equations can be derived from the Hamiltonian

$$\underline{K} = -\epsilon_x\underline{\rho}_x - \epsilon_y\underline{\rho}_y + A\underline{\rho}_x^{1/2}\underline{\rho}_y\left[\cos(\underline{\gamma}_x+2\underline{\gamma}_y)+\cos(\underline{\gamma}_x-2\underline{\gamma}_y)\right]. \tag{32}$$

This means that the motion corresponding to the point $\alpha(\nu_x-\frac{N}{2})$, $\alpha(\nu_y-\frac{N}{4})$ is the same as that for $(\nu_x-\frac{N}{2})$, $(\nu_y-\frac{N}{4})$ with the scaling law

$$\begin{aligned}
\theta &= \frac{1}{\alpha}\underline{\theta}, \\
\rho &= \alpha^2\underline{\rho}, \\
x &= \alpha\underline{x}, \\
y &= \alpha\underline{y}, \\
p_x &= \alpha\underline{p_x}, \\
p_y &= \alpha\underline{p_y}.
\end{aligned} \tag{33}$$

This means that motions are similar along any line through the intersection of the resonances in Fig. 1, with the coordinates scaling in proportion to the distance from the intersection and the time scaling in inverse proportion. Note that this result is rigorous, so long as the motion is adequately described by the Hamiltonian (32), and applies even to features which our analysis is unable to treat. By computing orbits along such a line for various values of α, it is possible to

find the distance $(\epsilon_x^2+\epsilon_y^2)^{1/2}$ from the intersection $\nu_x = \frac{N}{2}$, $\nu_y = \frac{N}{4}$ within which K represents the motion by comparing the stability limits and other properties of the orbits with the values scaled according to Eq. (33).

IV. Computed Orbit Studies

The motion was studied with the MURA I. B. M. 704 Computer using the ALGYTEE program written by M. Storm[5]. This computer program follows the motion by successively applying the transformation given by Eq. (3).

A series of three points were first examined. The results are given in Table I.

The initial conditions were $p_x \doteq 0$, and y, p_y very small. x_t is the value of x at which y growth occurs, and x_s the stability limit above which the motion grows to infinity. For $x_t < x < x_s$, the y amplitude grows to a finite amplitude and declines periodically. The instability for $x > x_s$, is a feature we have not yet treated in our analysis. According to the theorem of corresponding motion, the ratios x_s / x_{sL} and x_t / x_{tL} should be 9, 3, 1.

According to the above criteria, point 2 appears to be close enough to $\nu_x = \frac{N}{2}$, $\nu_y = \frac{N}{4}$ so that the other resonance lines were not perturbing the motion appreciably.

The point L was examined by L. J. Laslett[6]. For this point, x_s is very uncertain since the motion for this point is very erratic. A very small change in the initial conditions leads to very large and

TABLE I

	ν_x	ν_y	$\nu_x - \frac{1}{2}$	$\nu_y - \frac{1}{2}$	$\frac{\nu_x - \frac{1}{2}}{(\nu_x - \frac{1}{2})_L}$	x_s	$\frac{x_s}{x_{s\,L}}$	x_t	$\frac{x_t}{x_{t\,L}}$
L	.2200	.1150	-.2300	-.1350	9	.496	3.9	.331	9.5
1	.4230	.2048	-.0770	-.0452	3	.400	3.2	.110	3.2
2	.4744	.2350	-.0256	-.0150	1	.126	1.0	.0348	1.0

very erratic changes in the number of sectors for which the motion is stable. This may be because the point is almost as close to the $\nu_x + 2\nu_y = 0$ and $\nu_x = 0$ resonances as it is to the $\nu_x + 2\nu_y = N$ resonance. Thus, there are three resonances having nearly equal weight involved in the instability. It is almost on the $\nu_x - 2\nu_y = 0$ resonance which leads to growth, but not in itself to instability. Points 1 and 2 did not have this erratic behavior.

The insert in Fig. 1 shows a plot of eight points which were examined on the computer. They are all located on a semicircle at the same distance from $\nu_x = \frac{N}{2}$, $\nu_y = \frac{N}{4}$ as point 2 above. It is clear from the original Hamiltonian (1), and is also a consequence of the theorem of corresponding motions that the equations of motion are invariant under

$$\nu_x \rightarrow -\nu_x$$

$$\nu_y \rightarrow -\nu_y$$

$$x \rightarrow -x$$

$$y \rightarrow -y$$

$$p_x \rightarrow p_x$$

$$p_y \rightarrow p_y$$

Hence there is no additional information to be gained by taking points all the way around $\nu_x = \frac{N}{2}$, $\nu_y = \frac{N}{4}$. Table 2 shows the computed results, and the predicted values for these points. Fig. 3 shows the results in graphic form.

TABLE II

Point	ν_x	ν_y	Observed: Stability Limit	Observed: Threshold for y Growth	Theoretical: Limit for Absolute Stability x_ℓ	Theoretical: Threshold x_t, x_s
1	.52502	.26502	.126	.0350	.124	.0366
2	.51493	.27568	.249	.246	.213	.303
3	.48507	.27568	.246	.246	.0	.303
4	.47439	.26502	.0348	.035	.0	.0366
5	.47250	.26101	.0483	.048	.0	.0455
6	.47053	.25350	.270	.276	.0	.186
7	.47053	.24650	.305	.277	.0290	.186
8	.47250	.23900	.112	.0470	.0911	.0455

$$x_t = \frac{4\pi}{\lambda N} \left| \nu_x - 2\nu_y \right| \quad \text{for points 1, 2, 7, 8}$$

$$x_s = \frac{4\pi}{\lambda N} \left| \nu_x + 2\nu_y - N \right| \quad \text{for points 3, 4, 5, 6}$$

$$x_\ell = \frac{4\pi}{\lambda N} \left| \nu_y - \frac{N}{4} \right| \quad \text{for points 1, 2, 7, 8}$$

$$x_\ell = 0 \quad \text{for points 3, 4, 5, 6}$$

The results show the following:

1. In the first and third quadrants, (near the difference resonance), the effective stability limit is the greater of x_ℓ or x_t. For point 1, $x_\ell > x_t$ and x_ℓ is the effective stability limit. For point 2, $x_t > x_\ell$ and x_t is the effective stability limit. There is reason to believe that if the computer runs could be made long enough, points 7 and 8 would be found to have lower stability limits so that they too may fit into this picture. More will be said about 7 and 8 below.

2. If $x_t < x_\ell$, the y-amplitude grows to a finite amplitude and oscillates when $x_t < x < x_\ell$, while for $x_t > x_\ell$ y-growth leads to instability.

3. In the second and fourth quadrants (near the sum resonance) the theoretical stability limit x_s is the effective stability limit.

These results are consistent with the analytic theory. Near the sum resonance the analytic theory considering the sum resonance alone seems to give an adequate and complete treatment of the motion. Although it is "energetically" possible for the particle to escape, it does not in fact do so because there is another approximate constant of the motion (ρ_a) which prevents the particle from following the energy surface to infinity except when the stability limit is exceeded. Presumably the stability for $x < x_s$, at least well inside the second and fourth quadrants, should be as good as stability of non-linear motions in general as predicted by the Moser-Birkhoff methods. Experimentally,

we find that for one-dimensional motion, orbits within predicted stability limits are so stable, at least for the numbers of sectors we can now compute in a reasonable time, ($\sim 10^6$), that they do not deviate perceptibly (i.e. within as much one part in 10^5) from closed phase curves. For two-dimensional motion the orbits also appear stable for many sectors, but it is impossible to obtain as precise a measure of the stability because the phase motion is in four dimensions.

Near the difference resonance, our computed results are consistent with, but go beyond the analytic theory, and seem to suggest the following picture. Below the theoretical limit of stability x_ℓ, the motion is certainly stable, at least for very long times, and can be adequately accounted for by the analytic theory of the difference resonance alone, which gives a complete description of the motion. Above the limit x_ℓ, it is energetically possible for the particle to escape to infinity, but it will not in fact do so if we are below the threshold for coupling because the analytic theory, which should give a correct description at least for very long times, predicts that the particle remains near the x-axis and hence never arrives in the vicinity of the pass. However, above the coupling threshold, the particle wanders all over the energy surface, and hence finds its way out the pass and escapes. One consequence of this picture is that when $x_t > x_\ell$, a particle with x slightly greater than x_t has an energy well above the minimum ($-\frac{1}{2}H_\ell$) to cross the pass, and hence should quickly find its way out since the opening

available is large. However, if $x_t < x_\ell$, a particle with x slightly greater than x_ℓ has only barely enough energy to escape and must therefore strike the pass very accurately to escape. This is confirmed in part by the results which show that when $x_t > x_\ell$, the particle usually escapes immediately if $x > x_t$, whereas if $x_t < x_\ell$ and x is slightly above x_ℓ, the y-motion may grow and oscillate regularly a few times and even many times before suddenly going off to infinity. (By "infinity" we mean an amplitude large in comparison with the stable motion; the distinction is always very clear in that the particle coordinates all increase very rapidly when the motion becomes unstable.) This phenomenon is illustrated by the behavior at point 8 discussed below.

Computer runs for point 2 with initial conditions $p_x = p_y = 0$, $y = 10^{-8}$, x = .248 and .250, and for point 8 with initial x of .108, .116, .125, .133 are given in Table 3.

TABLE 3

Point	x Initial	Number of sectors before going unstable
2	.250	1,745
	.248	still stable at 10^6 sectors
8	.166	1,066
	.133	6,671
	.125	36,049
	.116,	346,620
	.108	still stable at 10^6 sectors

The stability limit for point 8 is not as sharply defined as that of point 2. If a series of computer runs of 25,000 sectors were made for

various values of initial x, and a second series of 10^6 sector runs were made, for point 2 one would find $.248 < x_s < .250$ for both runs, while for point 8 very different values would be found. If one could make runs of 10^9 sectors on point 8, x_s might be found to be much lower than the value given here. Points 1 through 6 behaved as point 2 above, and 7 and 8 like point 8. The behavior of point 7 is anomalous in view of the discussion above.

Point 8 shows the inadequacy of trying to study coupling resonances with runs of only a few hundred sectors.

In addition to the phenomena discovered here, which depend only on the two resonances, we may expect that if we move farther from the resonance, additional effects due to other resonances will arise. The neglected terms can be shown to cause rapid oscillations in the "constants" $\underline{K}$, ρ_2, etc., and when there are many of these, one might expect random fluctuations in their values. This would make predicted stability limits fuzzy and give rise to erratic behavior such as that observed by Laslett for point L (Table I). Note that this behavior is not what we have observed for point 8, although it resembles it, because point L is on the same ray, very nearly, as our point 1 which showed no such behavior; so that the erratic behavior at point L is a violation of the theorem of corresponding motions and must be due to neglected resonance terms.

LIST OF REFERENCES

1. See, e.g., R. Hagedorn, Stability of Two-Dimensional Non-Linear Oscillations with Periodical Hamiltonian. CERN Report PS/RH 9, November, 1955.
2. R. Hagedorn, Proceedings of the CERN Symposium on High Energy Accelerators and Pion Physics, Vol. 1, p. 293 (1956).
3. L. J. Laslett and K. R. Symon, Proceedings of the CERN Symposium on High Energy Accelerators and Pion Physics, Vol. 1, p. 279 (1956).
4. J. Moser, Nachr. Akad. Wiss. Göttingen, IIa, Nr. 6, p. 87.
5. M. R. Storm, ALGYTEE (Program 58). Midwestern Universities Research Association, Madison, 1957 (unpublished). Available on request. (MURA Report No. 233)
6. L. J. Laslett, Computational Examples of Solutions to Differential Equations which Simulate Growth of Axial Oscillations in an FFAG Accelerator Operated Near the $\sigma_x = 2\ \sigma_y$ Resonance. Midwestern Universities Research Association, Madison, 1957 (unpublished). Available on request. (MURA Report No. 295).

CAPTIONS FOR FIGURES

Fig. 1. Resonance diagram showing the resonances $\nu_x - 2\nu_y = 0$, $\nu_x + 2\nu_y = N$, and other important resonances influencing the motion. Insert shows working points for which digital computations were made.

Fig. 2. Phase plots for the Walkinshaw difference resonance $\nu_x - 2\nu_y = 0$. Shaded region is excluded as non-physical.

Fig. 3. Stability behavior of computed orbits near the intersection of the resonances $\nu_x - 2\nu_y = 0$, $\nu_x + 2\nu_y = N$. Initial x amplitude is plotted versus angular position α relative to the resonance lines in Fig. 1.

Dashed curves. Predicted threshold x_t for y-growth near difference resonance, and stability limit x_s below which motion must be stable.

Solid curve. Predicted limiting amplitude x_ℓ below which motion must be stable.

0 Observed threshold for y-growth.

+ Observed stability limit for growth to infinite amplitude.

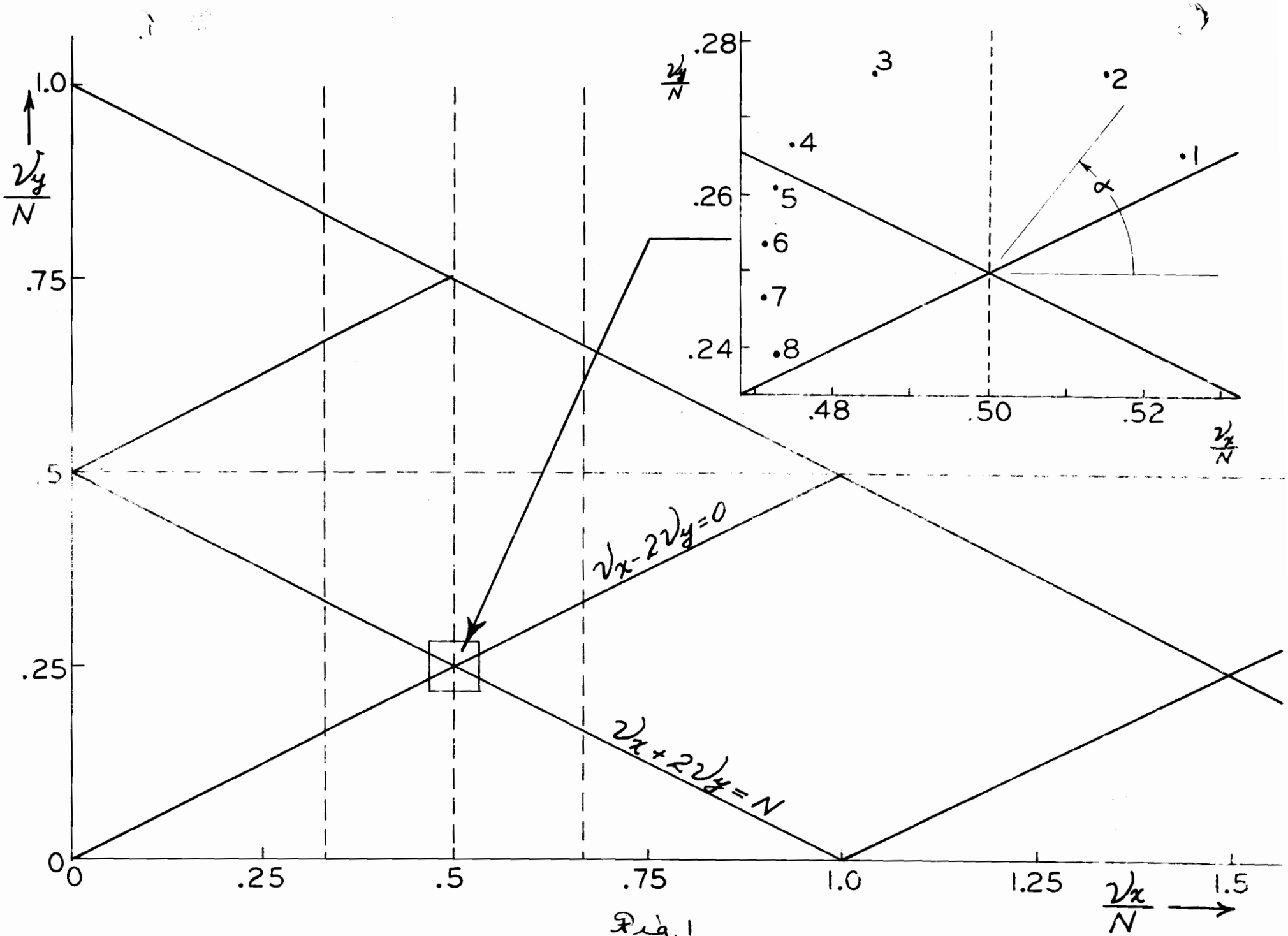
1.0
.75
.5
.25
0
$\frac{\nu_y}{N}$
0
.25
.5
.75
1.0
1.25
1.5
$\frac{\nu_x}{N}$
$\nu_x - 2\nu_y = 0$
$\nu_x + 2\nu_y = N$
.28
.26
.24
$\frac{\nu_y}{N}$
.48
.50
.52
$\frac{\nu_x}{N}$
.1
.2
.3
.4
.5
.6
.7
.8
α

Fig. 1

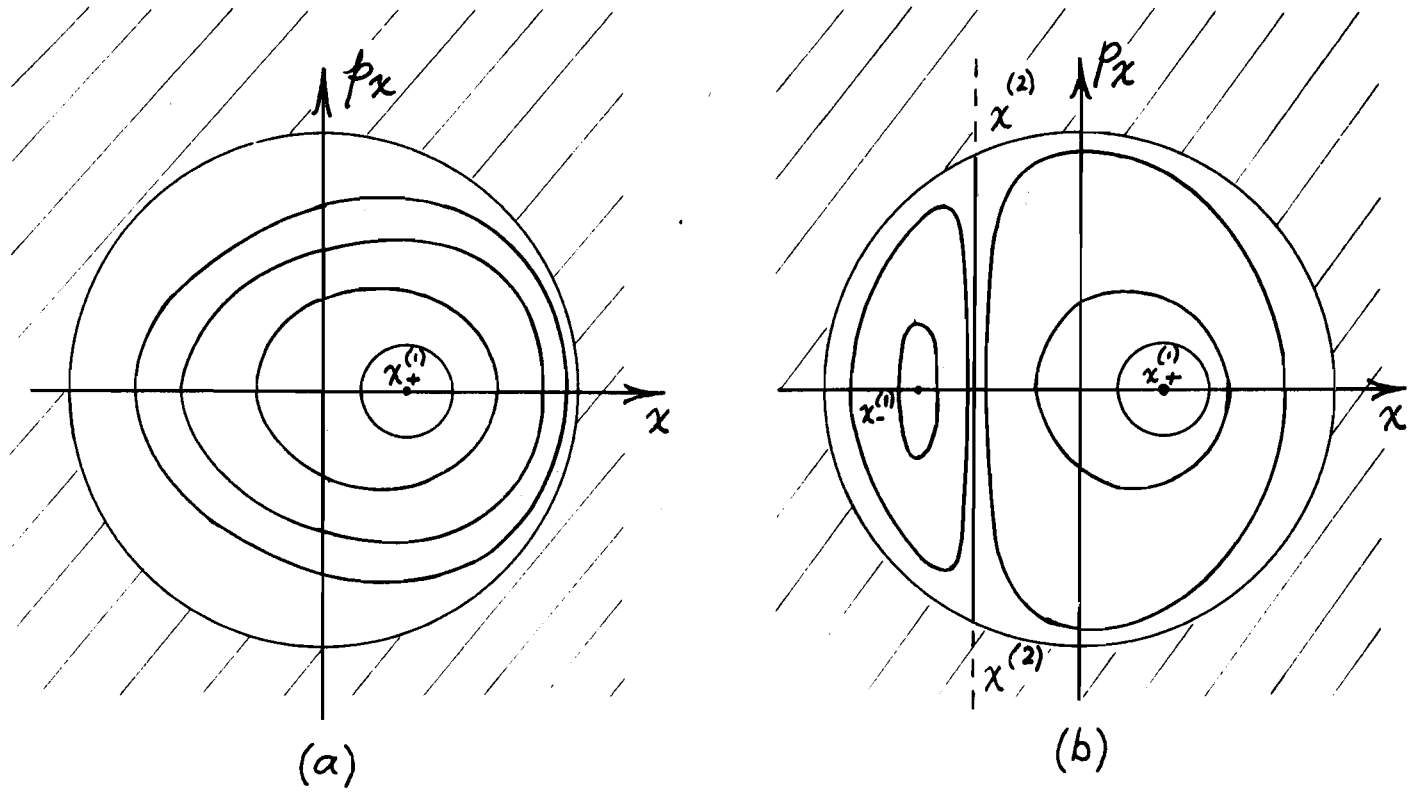

Fig. 2.

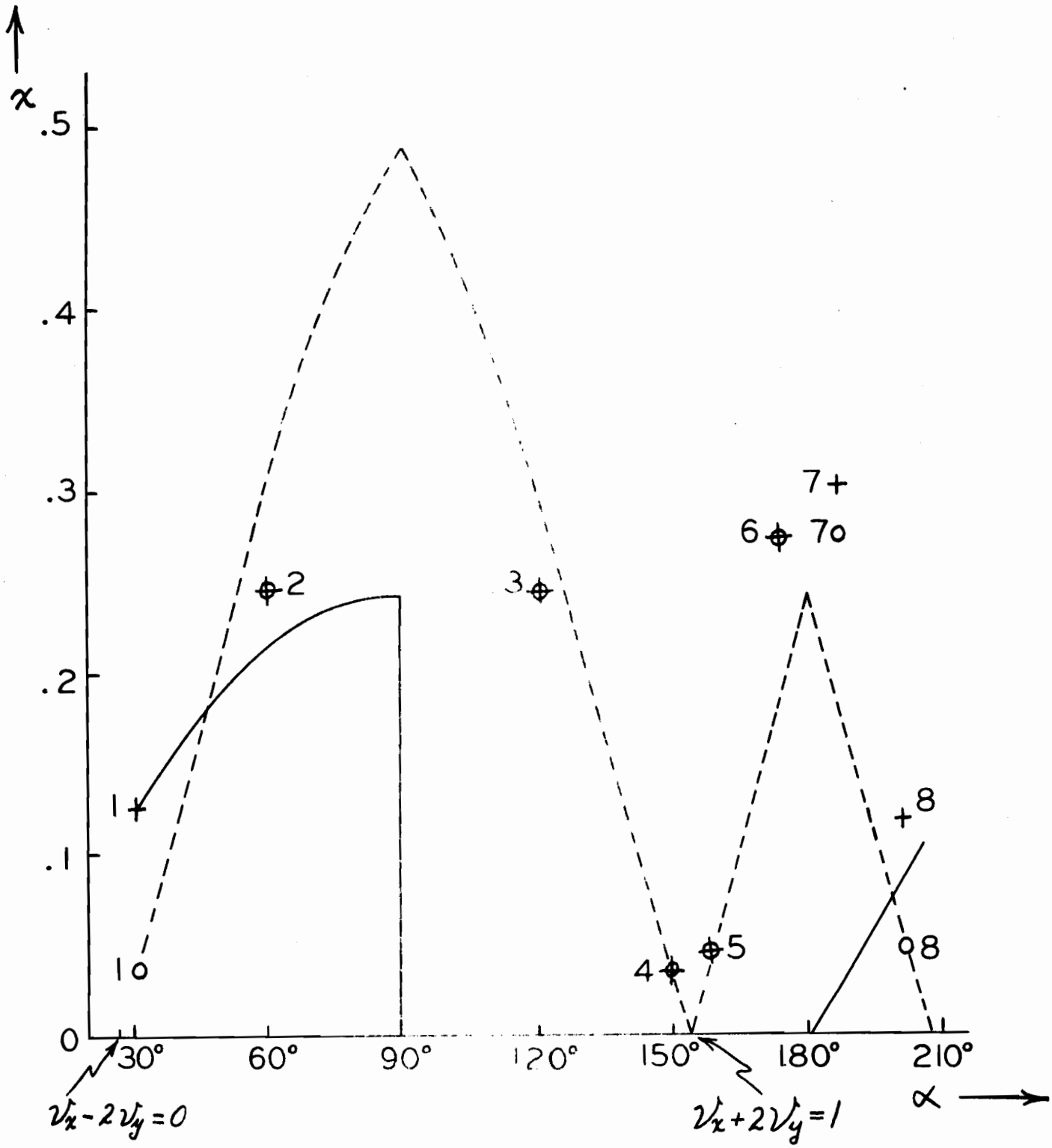
x
.5
.4
.3
.2
.1
0
30°
60°
90°
120°
150°
180°
210°
α
1
1
2
3
4
5
6
7
7
8
8
$\nu_x - 2\nu_y = 0$
$\nu_x + 2\nu_y = 1$

Fig. 3